IEEE TRANSACTIONS ON
EMERGING TOPICS
IN COMPUTING

Received 18 March 2013; revised 23 May 2013; accepted 29 June 2013. Date of publication 12 July 2013;
date of current version 20 September 2013.

Digital Object Identifier 10.1109/TETC.2013.2273218

Online Algorithm for Optimal Real-Time Energy Distribution in the Smart Grid

YU WANG, SHIWEN MAO (Senior Member, IEEE), AND R. M. NELMS (Fellow, IEEE)

Department of Electrical and Computer Engineering, Auburn University, Auburn, AL 36849-5201, USA
CORRESPONDING AUTHOR: S. MAO (smao@ieee.org)

This work was supported in part by the U.S. National Science Foundation under Grant CNS-0953513.

ABSTRACT The two-way energy and information flows in a smart grid, together with the smart devices, bring new perspectives to energy management and demand response. This paper investigates an online algorithm for electricity energy distribution in a smart grid environment. We first present a formulation that captures the key design factors such as user's utility and cost, grid load smoothing, dynamic pricing, and energy provisioning cost. The problem is shown to be convex and can be solved with an offline algorithm if future user and grid related information are known a priori. We then develop an online algorithm that only requires past and present information about users and the grid, and prove that the online solution is asymptotically optimal. The proposed energy distribution framework and the online algorithm are quite general, suitable for a wide range of utility, cost, and pricing functions. It is evaluated with trace-driven simulations and shown to outperform a benchmark scheme.

INDEX TERMS Convex optimization, demand response, electricity scheduling, online algorithm, smart grid.

I. INTRODUCTION

A. BACKGROUND AND MOTIVATION

A smart grid is an electrical grid that is enhanced with communications and networking, computing, and signal processing technologies [1]. Unlike the traditional power grid that is strictly hierarchical, the smart grid is characterized by the two-way flows of electricity and real-time information, which offers tremendous benefits and flexibility to both users and energy providers. With full-duplex information flows, configuration of the grid devices can be customized for timely response to the grid status. For example, energy storage systems can cooperate with distributed renewable energy resources (DRERs) to balance the supply and demand, and users can adapt their demand for energy according to the market price fluctuations [2].

The two-way energy and information flows, along with the smart devices, also bring new perspectives to energy management and demand response in the smart grid. Demand side management is one of the most important problems in smart grid research, which aims to match electricity demand to supply for enhanced energy efficiency and demand profile while considering user utility, cost and price [1]. Researchers have been focusing on peak shift or peak reduction for reducing the grid deployment and operational cost [3], [4], as well as on reducing user or energy provider's cost [5], [6]. In particular, some prior works aim to achieve a single objective, such as to improve the users' utility or reduce the cost of the energy provider [7], while others jointly consider both the user and energy provider costs, to increase the users' utility as much as possible while keeping the energy provider's cost at a relatively lower level [8]. Given the wide range of smart grid models and the challenge in characterizing the electricity demand and supply processes and the utility, cost, pricing functions, a general model that can accommodate various application scenarios would be highly desirable. Furthermore, it is important to jointly consider the utilities and costs of the key components of the system to achieve optimized performance for the overall smart grid system.

B. RELATED WORK

A comprehensive review on smart grid technologies and research can be found in [1], where the research on smart grid is classified into three major areas: infrastructure, management and protection. In the three areas, demand side management or demand response has been attracting considerable research efforts [2], [3], [5]–[11]. Researchers work mainly on demand profile shaping, user utility maximization and cost reduction. For example, machine learning is used in [5] to develop a learning algorithm for energy costs reduction and energy usage smoothing, while [7] aims to achieve a balance between user's cost and waiting time. In [8], the authors propose an optimal real-time pricing algorithm to maximize the social welfare, considering user utility maximization and energy provider cost minimization. In [10], the authors formulate a Stackelberg game between utility companies and end-users aiming to maximize the revenue of each utility company and the payoff of each user. In [11], the authors discuss the architecture of home machine-to-machine (M2M) networks for energy management, which is an important component in the smart grid. In these works, convex programming, machine learning and game theory are mostly used.

On the other hand, online algorithms [12] are widely used in wireless communications and networking, where precise channel and network information are hard to obtain. Recent research on solving wireless networking problems using online algorithms can be found in [13]–[16]. In [13], two online algorithms are developed from the optimal offline algorithms to maximize the amount of unit-length packets scheduled in a packet-switching mechanism. The authors of [14] address the energy-efficient uplink scheduling problem in a multiuser wireless system. With an online algorithm, an optimal scheduling is achieved without prior knowledge on arrival and channel statistics. In [15], online algorithm is applied to overcome the dynamic nature of the time-varying channels in wireless networks and then the throughput of the single-transmitter is maximized by optimal power assignment. In [16], online algorithm is used for multi-user video streaming in a wireless system so that user's perceived video quality and its variations are jointly considered for a maximization with almost no statistical information about the congested channels.

C. APPROACH

In this paper, we consider real-time energy distribution in a smart grid system. As shown in Fig. 1, the distribution control center (DCC) collects real-time information from the three key components, i.e., the users, the grid, and the energy provider, makes decisions on, e.g., electricity distribution, and then sends the decisions back to the key components to control their operations. The smart meters at the user side will be responsible for the information exchange with the DCC and for enforcing the electricity schedule received from the DCC. The information flows will be carried through a communications network infrastructure, such as a wireless network or a powerline communication system [1].

For optimizing the performance of such a complex network system, the utilities and costs of the three key components, i.e., the users, the grid, and the energy provider, should be jointly considered. In this paper, we take a holistic approach, to incorporate the key design factors including user's utility and cost, grid load smoothing, dynamic pricing, and energy

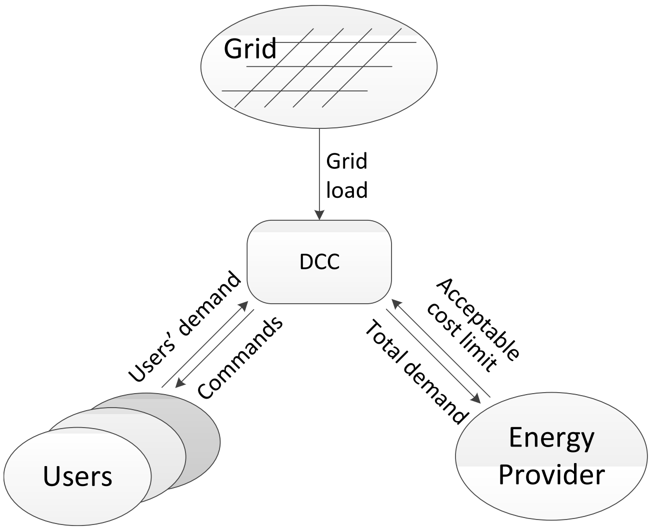

FIGURE 1. Illustration of the key elements and interactions in the smart grid.

provisioning cost in a problem formulation. To solve the real-time energy distribution problem, we first present an offline algorithm that can produce optimal solutions but assuming that the future user and grid information are known in advance. Based on the offline algorithm, we then develop an online algorithm that does not require any future information. As the name suggests, an online algorithm operates in an online setting, where the complete input is not known a priori [12]. It is very useful for solving problems with uncertainties [16]. We find the online algorithm particularly suitable in addressing the lack of accurate mathematical models and the lack of future information for electricity demand and supply in this problem. We also prove that the online algorithm converges to the optimal offline algorithm almost surely.

The proposed framework is quite general. It does not require any specific models for the electricity demand and supply processes, and only have some mild assumptions on the utility, cost, and price functions (e.g., convex and differentiable). The proposed algorithm can thus be applied to many different scenarios. The online algorithm also does not require any future information, making it easy to be implemented in a real smart grid system. It is also asymptotically optimal, a highly desirable property. Since there is no need for communications among the users, their privacy can be easily protected. The proposed algorithm is evaluated with trace-driven simulation using energy consumption traces recorded in the field. It outperforms a benchmark scheme that assumes global information.

D. ORGANIZATION

The remainder of this paper is organized as follows. We present the system model and problem formulation in Section II. The offline algorithm is introduced in Section III, and the online algorithm is developed and analyzed in Section IV. We present the simulation studies in Section V.

Section VI concludes this paper with a discussion future work.

II. PROBLEM STATEMENT

A. SYSTEM MODEL

1) NETWORK STRUCTURE

We consider a power distribution system in a smart grid environment where one energy provider supports the power usage of N users. The users could be residential, commercial and industrial energy consumers. Each user has a *smart meter* that manages the schedule of electrical devices [1]. We envisage that the smart meters could be a controller of electrical appliances in a house and are connected to the DCC of the energy provider through a communication network. At each time cycle, the smart meters update user information to, and receive control information from the DCC, while the DCC decides the power distribution among the users based on the real-time system information such as grid load, user demand and provider's cost. The DCC manages the entire system as a whole to achieve an optimum distribution scheme that balances the users' utility, supply cost of the energy provider, and the variance of the grid.

Here, the time cycles or slots indexed by $t \in \{1, 2, \ldots\}$ could be, e.g., 1 hour, 0.5 hour, 15 minutes and even shorter, according to the updating period of the smart meters and the size of the smart grid. Usually, the DCC takes a one-day operation cycle based on the daily periodical nature of electricity usage.[1] Let $\mathbb{N} = \{1, 2, \ldots, N\}$ be the set of users. We denote the power consumption of user i at time t as $p_i(t)$. At each time slot, user i's minimum demand $p_{i,min}(t)$ should be guaranteed, i.e.,

$$p_i(t) \geq p_{i,min}(t), \quad \forall\, i \in \mathbb{N}, t. \tag{1}$$

Besides, we assume that the users are rational, which means that at each time slot, power demand of each user has an upper bound, i.e., $p_i(t) \leq p_{i,max}(t)$. This will not become a constraint in our problem, because we aim to satisfy the user demand as much as possible under other constraints. However, this assumption together with (1) guarantees a closed set $\mathbb{P}$ which includes all the possible value of power demanded and used, that is, $p_i(t) \in \mathbb{P}$.

2) USER UTILITY FUNCTION

We assume independent users with their own preferences of power usage. For example, each user could have its own time schedule for using different electrical appliances. Also, the user demand may vary as weather changes. Usually the power consumption is larger in a hot summer day than that in a mild day in the spring. Besides, different users may have different reactions to different price schemes [6]. Therefore, it is difficult to characterize user preference with a precise mathematical model. In prior work, user preference is usually represented by a *utility function* [5]. Similarly, we use function $U(p_i(t), \omega_i(t))$ to represent user i's satisfaction on power consumption. We assume $U(\cdot, \cdot)$ to be a strictly increasing, concave function of the allocated power $p_i(t)$; its form could be general. One example is the widely used quadratic utility function [5], [6], [8]. For each user i, the other parameter $\omega_i(t)$ of the utility function indicates the user's flexibility at time t. A larger $\omega_i(t)$ means higher flexibility. $\omega_i(t)$ could be different for users or vary over time. Its values are sent to the DCC at each updating cycle by the smart meter.

3) ENERGY PROVISIONING COST

For energy providers, when demand is in the normal level, the generation cost increases only slowly as the demand grows. However, it will cost much more when the load peak is approaching the grid capacity, because the provider has to transmit more power from the outside or backup batteries to avoid a blackout. Therefore, we use an increasing and strictly convex function to approximate the *cost function* for energy provisioning. Similar to [6], [8], we choose a quadratic function to model the provider's cost.

$$C(L(t)) = a \cdot L^2(t) + b \cdot L(t) + c, \tag{2}$$

where $a > 0$ and $b, c \geq 0$ are pre-selected for the power grid and $L(t) = \sum_{i \in \mathbb{N}} p_i(t)$ denotes the grid load, i.e., the total power consumption for time slot t. From the provider's perspective, we assume that it aims to meet the user demand under an acceptable cost constraint $c(t)$ at time t, which shall not be exceeded.

$$C(L(t)) \leq c(t), \quad \forall\, t \in \{1, 2, \ldots, T\}. \tag{3}$$

We call $c(t)$ *budget* in the rest of this paper. Without loss of generality, we assume $c(t)$ to be a stationary ergodic process, which is taken from a set $\mathbb{C}$, i.e., $c(t) \in \mathbb{C}$.

4) PRICE MODEL

Dynamic pricing like real-time pricing (RTP), critical peak pricing (CPP) and time of use pricing (TUP) [17] could be incorporated in the smart grid environment. However, real electricity market is still dominated by simple pricing schemes. In this paper, we use a simple price model that can characterize most real electricity markets, especially for residential usage. As shown in [4], [18], without dynamic price demand, the price load curve has the shape of a *hockey stick*; it remains flat over a long range of grid load and then grows upward steeply as demand approaches the grid capacity. Let $f(\cdot)$ be the *price function* and $f(L(t))$ the price at time t. Therefore, we assume $f(\cdot)$ to be a twice-differentiable increasing convex function that maps the total load to a price. Similar to the utility function $U(\cdot)$, the price function $f(\cdot)$ could have a general form as well.

B. PROBLEM FORMULATION

As mentioned in Section I, we aim to minimize the load variance in the grid while maximizing user satisfaction. Large

[1]Note that this is not a requirement for the model and the proposed algorithms, but a typical scenario in most practical cases, which will be applied in the simulation studies.

load variance is undesirable for grid operation. It brings about uncertainties that affect not only user satisfaction but also the stability of the power system. Furthermore, the energy provisioning cost should be bounded and users' necessary power needs should be guaranteed.

We first consider an offline scenario where the DCC distributes the power to users during time $t = 1, 2, \ldots, T$, and all the information on users' flexibility $\omega_i(t)$ and provider's budget $c(t)$ are assumed to be known in advance. Let $P_i(t)$ denote the power usage for user i at time t, for $t \in \{1, 2, \ldots, T\}$. In this paper, we use upper case P in the *offline problem* (see Section III), where all the necessary constraints are known a priori. In the corresponding *online problem*, which will be examined in Section IV, we use lower case p for the corresponding variables. A vector with subscript i is used to denote a time sequence, e.g., $\vec{P}_i$ for the power usage by user i for $t \in \{1, 2, \ldots, T\}$. The offline problem can be formulated as follows:

$$\max: \sum_{t=1}^{T}\sum_{i\in\mathbb{N}}\left[U(P_i(t),\omega_i(t)) - f\left(\sum_{i\in\mathbb{N}}P_i(t)\right)P_i(t)\right] - \frac{\alpha T}{2}\mathrm{Var}\left(\sum_{i\in\mathbb{N}}\vec{P}_i\right) \quad (4)$$

subject to:

$$P_i(t) \geq P_{i,min}(t), \quad \forall\, i \in \mathbb{N}, t \in \{1, 2, \cdots, T\} \quad (5)$$

$$C\left(\sum_{i\in\mathbb{N}}P_i(t)\right) \leq c(t) \quad \forall\, t \in \{1, 2, \cdots, T\}, \quad (6)$$

where

$$\mathrm{Var}\left(\sum_{i\in\mathbb{N}}\vec{P}_i\right) = \frac{1}{T}\sum_{t=1}^{T}\left(\sum_{i\in\mathbb{N}}P_i(t) - \frac{1}{T}\sum_{k=1}^{T}\sum_{i\in\mathbb{N}}P_i(k)\right)^2.$$

The objective function (4) consists of two parts. The first part represents users' satisfaction and preference as the difference between user utility and cost. The second part represents the load variance of the grid. These two parts are integrated with a parameter $\alpha > 0$, allowing a trade-off between the two. Constraint (5) indicates the minimum user demand should be guaranteed, while constraint (6) represents the cost upper bound for the energy provider. In section III, we present an algorithm that can solve this offline problem and explain how we can move from offline to online. In Section IV, we present an algorithm to solve the corresponding online problem that does not require any a priori user/grid information, and show that the online algorithm is asymptotically optimal.

III. OFFLINE ALGORITHM

In the offline problem (4), the user power consumption $P_i(t)$'s are independent. Hence the variance term can be rewritten as $\mathrm{Var}\left(\sum_{i\in\mathbb{N}}\vec{P}_i\right) = \sum_{i\in\mathbb{N}}\mathrm{Var}(\vec{P}_i)$ and the *price function* $f\left(\sum_{i\in\mathbb{N}}P_i(t)\right)$ is the same for each user, which means that $\sum_{i\in\mathbb{N}}f\left(\sum_{i\in\mathbb{N}}P_i(t)\right)P_i(t) = f\left(\sum_{i\in\mathbb{N}}P_i(t)\right)\sum_{i\in\mathbb{N}}P_i(t)$. Therefore, we rewrite the price term and variance term respectively. Then the problem can be reformulated as follows (termed Prob-OFF).

$$\max: \Psi(\mathbf{P}) = \sum_{t=1}^{T}\sum_{i\in\mathbb{N}}U(P_i(t),\omega_i(t)) - \sum_{t=1}^{T}f\left(\sum_{i\in\mathbb{N}}P_i(t)\right)\sum_{i\in\mathbb{N}}P_i(t) - \frac{\alpha T}{2}\sum_{i\in\mathbb{N}}\mathrm{Var}\left(\vec{P}_i\right) \quad (7)$$

subject to: (5) − (6),

where $\mathbf{P}$ is an $N \times T$ matrix that denotes the power allocated for each user i at time $t \in \{1, 2, \ldots, T\}$ and $\mathrm{Var}(\vec{P}_i) = \frac{1}{T}\sum_{t=1}^{T}\left(P_i(t) - \frac{1}{T}\sum_{k=1}^{T}P_i(k)\right)^2$.

In Prob-OFF, $U(\cdot)$ is concave and $C(\cdot)$ is convex. Since the price function $f(\cdot)$ is convex, $f(\sum_{i\in\mathbb{N}}P_i(t))\sum_{i\in\mathbb{N}}P_i(t)$ is also convex. We only need to show the convexity of $\mathrm{Var}(\vec{P}_i)$ to establish a convex optimization problem. The convexity of $\mathrm{Var}(\vec{P}_i)$ can be easily proved by its definition.

Lemma 1: Prob-OFF is a convex optimization problem and has a unique solution.

Proof: For two vectors $\vec{P}_i^1$, $\vec{P}_i^2$ and for any $i \in \mathbb{N}$, $0 < \theta < 1$, it follows from the variance definition and the strict convexity of quadratic function $f(x) = x^2$ that

$$\mathrm{Var}(\theta\vec{P}_i^1 + (1-\theta)\vec{P}_i^2) \leq \theta\mathrm{Var}(\vec{P}_i^1) + (1-\theta)\mathrm{Var}(\vec{P}_i^2).$$

We conclude that $\mathrm{Var}(\vec{P}_i)$ is strictly convex unless $\mathrm{Var}(\vec{P}_i^1) = \mathrm{Var}(\vec{P}_i^2)$. Since all the constraints of Prob-OFF are also convex, we conclude that Prob-OFF is a convex problem.

We next prove that Prob-OFF has a unique solution. Assume $\vec{P}_i^1$ and $\vec{P}_i^2$ are two optimal solutions to Prob-OFF. Because the objective function is concave, $\theta\vec{P}_i^1 + (1-\theta)\vec{P}_i^2$ is also optimal, for $0 < \theta < 1$. Note that we have three terms that are all concave (or convex) in (7). Thus $\theta\vec{P}_i^1 + (1-\theta)\vec{P}_i^2$ is optimal only if

$$U(\theta P_i^1(t)+(1-\theta)P_i^2(t)) = \theta U(P_i^1(t))+(1-\theta)U(P_i^2(t)) \quad (8)$$

$$f\left(\theta\vec{P}_i^1 + (1-\theta)\vec{P}_i^2\right)\cdot\left(\theta\sum_{i\in\mathbb{N}}P_i^1(t) + (1-\theta)\sum_{i\in\mathbb{N}}P_i^2(t)\right) = \theta f(\vec{P}_i^1)\sum_{i\in\mathbb{N}}P_i^1(t) + (1-\theta)f(\vec{P}_i^2)\sum_{i\in\mathbb{N}}P_i^2(t) \quad (9)$$

$$\mathrm{Var}(\theta\vec{P}_i^1+(1-\theta)\vec{P}_i^2) = \theta\mathrm{Var}(\vec{P}_i^1)+(1-\theta)\mathrm{Var}(\vec{P}_i^2) \quad \forall\, i \in \mathbb{N}. \quad (10)$$

Since $U(\cdot)$ is assumed to be a strictly increasing function in Section II-A.2, (8) holds true if and only if $P_i^1(t) = P_i^2(t)$, for all $i \in \mathbb{N}$, $t \in \{1, 2, \ldots, T\}$. Eqs. (9) and (10) are also sufficient for this result. Therefore, we conclude that Prob-OFF is a convex problem with a unique solution. ■

As Lemma 1 holds, we can carefully choose $P_{i,min}(t)$ to meet Slater's condition [19], and thus the KKT conditions [19] are sufficient and necessary for the optimality of Prob-OFF. Let $\mathbf{P}^*$ be an optimal solution to Prob-OFF.

Let $\eta(t)$ and $\gamma_i(t)$ be the Lagrange multipliers and variables, respectively, for $i \in \mathbb{N}$ and $t \in \{1, 2, \cdots, T\}$. We have

$$\begin{cases} U'(P_i^*(t), \omega_i(t)) - h\left(\sum_{i\in\mathbb{N}} P_i^*(t)\right) - \alpha\left(P_i^*(t) - \bar{P}_i^*\right) \\ \qquad -\eta(t)C'\left(\sum_{i\in\mathbb{N}} P_i^*(t)\right)/c(t) + \gamma_i(t) = 0 \\ \eta(t)\left(C\left(\sum_{i\in\mathbb{N}} P_i^*(t)\right)/c(t) - 1\right) = 0 \\ \gamma_i(t)\left(P_i^*(t) - P_{i,min}(t)\right) = 0 \\ \eta(t), \gamma_i(t) \geq 0, \forall\, i \in \mathbb{N},\ t \in \{1, 2, \cdots, T\}, \end{cases} \tag{11}$$

where

$$h\left(\sum_{i\in\mathbb{N}} P_i^*(t)\right) = f'\left(\sum_{i\in\mathbb{N}} P_i^*(t)\right)\sum_{i\in\mathbb{N}} P_i^*(t) + f\left(\sum_{i\in\mathbb{N}} P_i^*(t)\right)$$

and

$$\bar{P}_i^* = \frac{1}{T}\sum_{k=1}^{T} P_i^*(k). \tag{12}$$

From the above equations, we can solve for $\eta(t)$ as

$$\eta(t) = \left(\alpha\left(\bar{P}_i^* - P_i^*(t)\right) + U'(P_i^*(t), \omega_i(t)) - \left(h\left(\sum_{i\in\mathbb{N}} P_i^*(t)\right) + \gamma_i(t)\right)\right) \Big/ \left(C'\left(\sum_{i\in\mathbb{N}} P_i^*(t)\right)/c(t)\right). \tag{13}$$

Therefore, to achieve optimality, there is an identical $\eta(t)$ for all users in a time slot t. The optimal solution guarantees that the right-hand-side (RHS) of (13) has the same value for all users. Furthermore, we observe that only the $\bar{P}_i^*$ term requires information from other time slots. This implies that if $\bar{P}_i^*$ could be accurately estimated, the optimal energy distribution P^* could be determined using only information in the current time slot, such as $c(t)$ and $P_{i,min}(t)$. This is essential, because in the offline scenario, our assumption that future information are known a priori is not a possible case in the real smart grid. Based on this observation, we are able to present an *online algorithm* for the energy distribution problem in the next section which requires no future information.

IV. ONLINE ALGORITHM

In this section, we present an online algorithm for energy distribution, and prove that the online solution is asymptotically convergent to the offline optimal solution, i.e., *asymptotically optimal*. The online energy distribution algorithm consists of the following three steps.

Step 1: For each $i \in \mathbb{N}$, initialize $\hat{p}_i(0) \in \mathbb{P}$.

Step 2: In each time slot t, the DCC solves the following convex optimization problem (termed Prob-ON).

$$\text{max:}\ \sum_{i\in\mathbb{N}} U(p_i(t), \omega_i(t)) - f\left(\sum_{i\in\mathbb{N}} p_i(t)\right)\sum_{i\in\mathbb{N}} p_i(t) - \frac{\alpha}{2}\sum_{i\in\mathbb{N}}(p_i(t) - \hat{p}_i(t-1))^2 \tag{14}$$

$$\text{subject to:}\ p_i(t) \geq p_{i,min}(t), \quad \forall\, i \in \mathbb{N} \tag{15}$$

$$C\left(\sum_{i\in\mathbb{N}} p_i(t)\right) \leq c(t), \quad \forall\, t. \tag{16}$$

Let $\vec{p}^*(t)$ denote the solution to Prob-ON, where each element $p_i^*(t)$ represents the optimal power allocation to user i.

Step 3: Update $\hat{p}_i(t)$ for all $i \in \mathbb{N}$ as follows.

$$\hat{p}_i(t) = \hat{p}_i(t-1) + \frac{\alpha}{t+\alpha}\cdot(p_i^*(t) - \hat{p}_i(t-1)). \tag{17}$$

$\vec{p}^*(t)$ is indeed the short term of $\vec{p}^*(\hat{\vec{p}}, c(t))$. For brevity, we use $\vec{p}^*(t)$ instead in the paper when it is clear in context. Comparing to (7), the variance term is approximated by $\sum_{i\in\mathbb{N}}(p_i(t) - \hat{p}_i(t-1))^2$ in (14). In Prob-ON, (17) can be viewed as a stochastic approximation updating equation, if the budget of the energy provider, $c(t)$, is viewed as a stationary stochastic process. This interpretation can be justified because $c(t)$ is assumed to be stationary and ergodic.

Similar to Prob-OFF, problem Prob-ON is also a convex optimization problem satisfying Slater's condition. Its KKT conditions with KKT multipliers $\lambda(t)$ and KKT variables $\nu_i(t)$, for $i \in \mathbb{N}$, are as follows.

$$\begin{cases} U'(p_i^*(t), \omega_i(t)) - h\left(\sum_{i\in\mathbb{N}} p_i^*(t)\right) - \alpha\left(p_i^*(t) - \hat{p}_i(t-1)\right) \\ \qquad -\lambda(t)C'\left(\sum_{i\in\mathbb{N}} p_i^*(t)\right)/c(t) + \nu_i(t) = 0 \\ \lambda(t)\left(C\left(\sum_{i\in\mathbb{N}} p_i^*(t)\right)/c(t) - 1\right) = 0 \\ \nu_i(t)\left(p_i^*(t) - p_{i,min}(t)\right) = 0 \\ \lambda(t), \nu_i(t) \geq 0, \quad \forall\, i, t. \end{cases} \tag{18}$$

In the remainder of this section, we firstly prove that $\hat{p}_i(t)$ approaches a limit for t goes to infinity and then we show that $\hat{p}_i(t)$ converges to the mean of the power allocated to each user $i \in \mathbb{N}$ over time, as given in (12).

We begin with the definition the function $g(\hat{\vec{p}}, c(t))$:

$$g(\hat{\vec{p}}, c(t)) = \sum_{i\in\mathbb{N}} U(p_i^*(\hat{\vec{p}}, c(t)), \omega_i(t)) - f\left(\sum_{i\in\mathbb{N}} p_i^*(\hat{\vec{p}}, c(t))\right)\sum_{i\in\mathbb{N}} p_i^*(\hat{\vec{p}}, c(t)) - \frac{\alpha}{2}\sum_{i\in\mathbb{N}}(p_i^*(\hat{\vec{p}}, c(t)) - \hat{p}_i)^2. \tag{19}$$

Note that the optimized function $g(\hat{\vec{p}}, c(t))$ share the same form with (14), but with a different meaning. Here we regard the optimizer $\vec{p}^*(\hat{\vec{p}}, c(t))$ and the optimized objective $g(\hat{\vec{p}}, c(t))$ as stochastic processes. We need to show the process $\hat{\vec{p}}(t)$ converges almost surely, for given stationary stochastic process $c(t)$. We have the following immediate properties of $\vec{p}^*(\hat{\vec{p}}, c(t))$ and $g(\hat{\vec{p}}, c(t))$.

Property 1: Continuity of $\vec{p}^*(\hat{\vec{p}}, c(t))$ and $g(\hat{\vec{p}}, c(t))$. For any $c(t) \in \mathbb{C}$, we have
i) $\vec{p}^*(\hat{\vec{p}}, c(t))$ and $g(\hat{\vec{p}}, c(t))$ are continuous functions of $\hat{\vec{p}}$;
ii) $E[\vec{p}^*(\hat{\vec{p}}, c(t))]$, $E[g(\hat{\vec{p}}, c(t))]$ are continuous functions of $\hat{\vec{p}}$.

Proof: i) From (14), $g(\hat{\vec{p}}, c(t))$ is a continuous function of $\hat{\vec{p}}$. The continuity of $\vec{p}^*(\hat{\vec{p}}, c(t))$ could be guaranteed if all the four conditions of Theorem 2.2 from [20] are satisfied. The conditions are verified because Prob-ON is always feasible on a closed set and $\hat{\vec{p}}$ is bounded on a set $\mathbb{P}$ in our case. Therefore, $\vec{p}^*(\hat{\vec{p}}, c(t))$ is continuous with respect to $\hat{\vec{p}}$.

ii) Take $\hat{\vec{p}}_n$ as any sequence such that $\lim_{n\to\infty} \hat{\vec{p}}_n = \hat{\vec{p}}$. Then we have

$$\lim_{m\to\infty} E[p_i^*(\hat{\vec{p}}_n, c(t))] = E[\lim_{m\to\infty} p_i^*(\hat{\vec{p}}_n, c(t))] = E[p_i^*(\hat{\vec{p}}, c(t))],$$

which follows the Bounded Convergence Theorem (see [21]) since we already have the continuity of $\vec{p}^*(\hat{\vec{p}}, c(t))$ and the closed set $\mathbb{P}$ of p_i^* (see II-A.1). Consequently, $E[g(\hat{\vec{p}}, c(t))]$ is also continuous. ∎

Property 2: Differentiability of $g(\hat{\vec{p}}, c(t))$ and $E[g(\hat{\vec{p}}, c(t))]$. For any $c(t) \in \mathbb{C}$ and each $i \in \mathbb{N}$, we have
i) $\nabla_{\hat{p}_i} g(\hat{\vec{p}}, c(t)) = \alpha(p_i^*(\hat{\vec{p}}, c(t)) - \hat{p}_i)$;
ii) $\nabla_{\hat{p}_i} E[g(\hat{\vec{p}}, c(t))] = \alpha(E[p_i^*(\hat{\vec{p}}, c(t))] - \hat{p}_i)$.

Proof: i) The differentiability of $g(\hat{\vec{p}}, c(t))$ follows directly from Theorem 4.1 in [22].

ii) Similar to the proof in Part ii) of Property 1, take any sequence $\hat{p}_{i,n}$ such that $\lim_{n\to\infty} \hat{p}_{i,n} = 0$. We have that $\left|\frac{g(\hat{\vec{p}}+\hat{p}_{i,n}\vec{e})-g(\hat{\vec{p}},c(t))}{\hat{p}_{i,n}}\right| = \alpha \left|p_i^*(\hat{\vec{p}} + p_{0,n}\vec{e}, c(t)) - \hat{p}_i - p_{0,n}\right| \le \alpha p_{max}$, for $0 < p_{0,n} < \hat{p}_{i,n}$, which follows the Mean Value Theorem and part (ii) of Property 2. For each $i \in \mathbb{N}$,

$$\begin{aligned}\frac{\partial}{\partial \hat{p}_i} E[g(\hat{\vec{p}}, c(t))] &= \lim_{n\to\infty} E\left[\frac{g(\hat{\vec{p}} + \hat{p}_{i,n}\vec{e}) - g(\hat{\vec{p}}, c(t))}{\hat{p}_{i,n}}\right] \\ &= E\left[\lim_{n\to\infty} \frac{g(\hat{\vec{p}} + \hat{p}_{i,n}\vec{e}) - g(\hat{\vec{p}}, c(t))}{\hat{p}_{i,n}}\right] \\ &= \alpha(E[p_i^*(\hat{\vec{p}}, c(t))] - \hat{p}_i).\end{aligned}$$

∎

With Properties 1 and 2, we are able to show the following result, which is an important step to the proof of the convergence of process $\hat{\vec{p}}$.

Lemma 2: The solution of the following fixed point equation is unique

$$E[\vec{p}^*(\hat{\vec{p}}, c(t))] = \hat{\vec{p}}. \tag{20}$$

Proof: We define several notations to be used in this proof. Define $\rho_i = \sqrt{\alpha} p_i$ and $\rho_i^*(\hat{\vec{\rho}}, c(t)) = \sqrt{\alpha} p_i^*(\hat{\vec{p}}, c(t))$ for each $i \in \mathbb{N}$ and $p_i \in \mathbb{P}$, and function $\vec{\rho}_i{}^*(\hat{\vec{\rho}}, c(t))$. Also define $\text{dist}(\vec{p}^1, \vec{p}^2) = \sqrt{\sum_{i\in\mathbf{N}}(p_i^1 - p_i^2)^2} = \left|\sum_{i\in\mathbf{N}}(p_i^1 - p_i^2)\right|$, for any $\vec{p}^1, \vec{p}^2 \in \mathbb{P}^N$.

We next show the following two intermediate results that will be used to prove the lemma. The first result is that the solution of the next fixed point equation exits.

$$E[\vec{\rho}_i{}^*(\hat{\vec{\rho}}, c(t))] = \hat{\vec{\rho}}. \tag{21}$$

It follows Property 1 that $E[\vec{\rho}_i{}^*(\hat{\vec{\rho}}, c(t))]$ is a continuous function and it maps a convex compact subset of $\mathbb{P}^N$ to itself. Hence from Brouwer's Fixed Point Theorem in [23], the existence of the solution to (21) can be shown.

Secondly, we show that $E[\vec{\rho}_i{}^*(., c(t))]$ is a pseudo-contraction. Since $\mathbb{P}^N$ is a compact set, we need to show equivalently that for any two different $\hat{\vec{p}}^1$and $\hat{\vec{p}}^2 \in \mathbb{P}^N$,

$$\text{dist}(E[\vec{\rho}_i{}^*(\hat{\vec{\rho}}^1, c(t))], E[\vec{\rho}_i{}^*(\hat{\vec{\rho}}^2, c(t))]) < \text{dist}(\hat{\vec{\rho}}^1, \hat{\vec{\rho}}^2).$$

Here, let $\hat{\vec{\rho}}^1$ be a solution to (21) and $\hat{\vec{\rho}}^2 \neq \hat{\vec{\rho}}^1$.

To prove this, we modify the Prob-ON to obtain a new problem New-Prob-ON as

$$\begin{aligned} \max: \quad & g_0(\vec{\rho}, \hat{\vec{\rho}}) \\ \text{subject to:} \quad & \frac{\rho_i}{\sqrt{\alpha}} \ge p_{i,min} \forall\, i \in \mathbb{N} \\ & C\left(\sum_{i\in\mathbb{N}} \frac{\rho_i}{\sqrt{\alpha}}\right) \le c(t), \quad \forall\, t, \end{aligned} \tag{22}$$

where $g_0(\vec{\rho}, \hat{\vec{\rho}}) = \sum_{i\in\mathbb{N}} U(\frac{\rho_i}{\sqrt{\alpha}}, \omega_i) - f(\sum_{i\in\mathbb{N}} \frac{\rho_i}{\sqrt{\alpha}}) \sum_{i\in\mathbb{N}} \frac{\rho_i}{\sqrt{\alpha}} - \frac{\alpha}{2} \sum_{i\in\mathbb{N}}(\frac{\rho_i}{\sqrt{\alpha}} - \frac{\hat{\rho}_i}{\sqrt{\alpha}})^2$. For brevity, we drop the time index (t) in the remainder of this proof, when their meanings are clear in the context. Note that $\vec{\rho}_i{}^*(\hat{\vec{\rho}}, c(t))$ is the optimal solution for New-Prob-ON.

Now, we use Proposition 6.1 from [22] to achieve the Lipschitz continuity and acquire the Lipschitz constant of $\vec{\rho}_i{}^*(., c(t))$ in a neighborhood of $\hat{\vec{\rho}}^1$. Two conditions are necessary to hold the proposition: the Lipschitz continuity of the difference function in a neighborhood of $\hat{\vec{\rho}}^1$ and the second-order growth condition.

We define the difference function $\Delta g_0(\vec{\rho}, \hat{\vec{\rho}}^1, \hat{\vec{\rho}}^2)$ as

$$\begin{aligned}\Delta g_0(\vec{\rho}, \hat{\vec{\rho}}^1, \hat{\vec{\rho}}^2) &= g_0(\vec{\rho}, \hat{\vec{\rho}}^2) - g_0(\vec{\rho}, \hat{\vec{\rho}}^1) \\ &= \frac{1}{2} \sum_{i\in\mathbb{N}} (\hat{\rho}_i^1 - \hat{\rho}_i^2)(2\rho_i - \hat{\rho}_i^1 - \hat{\rho}_i^2).\end{aligned}$$

Then it follows that

$$\begin{aligned}&\text{dist}(\Delta g_0(\vec{\rho}^1, \hat{\vec{\rho}}^1, \hat{\vec{\rho}}^2), \Delta g_0(\vec{\rho}^2, \hat{\vec{\rho}}^1, \hat{\vec{\rho}}^2)) \\ &= \left|\sum_{i\in\mathbb{N}} (\hat{\rho}_i^1 - \hat{\rho}_i^2)(\rho_i^1 - \rho_i^2)\right| \le \text{dist}(\hat{\vec{\rho}}^1, \hat{\vec{\rho}}^2)\text{dist}(\vec{\rho}^1, \vec{\rho}^2),\end{aligned} \tag{23}$$

where the inequality holds from Cauchy-Schwarz inequality. Hence, the first condition of Proposition 6.1 in [22] holds.

Next, we show that the second condition also holds. In our case, the second-order growth condition requires that there exists a positive constant a such that

$$g_0(\vec{\rho}^*(\hat{\vec{\rho}}^1, c(t)), \hat{\vec{\rho}}^1) - g_0(\vec{\rho}, \hat{\vec{\rho}}^1) \geq a(\text{dist}(\vec{\rho}, \vec{\rho}^*(\hat{\vec{\rho}}^1, c(t))))^2.$$

We find a sufficient condition for this second-order growth condition in [24], in which Theorem 6.1 states that if the Slater qualification hypothesis holds, the second-order growth condition (Theorem 6.1 (v)) is equivalent with three other conditions (Theorem 6.1 (vi)−(viii)). Because the Slater qualification hypothesis could be satisfied if we carefully choose $p_{i,min}$ (see Section III). We thus verify that an equivalent condition Theorem 6.1 (vii) is satisfied. For this, define:

$$\begin{aligned} &L(\vec{\rho}, \lambda, (\nu_i : i \in \mathbb{N})) \\ &= g_0(\vec{\rho}^*(\hat{\vec{\rho}}^1, c(t)), \hat{\vec{\rho}}^1) - g_0(\vec{\rho}, \hat{\vec{\rho}}^1) \\ &+\lambda\left(\frac{1}{c(t)}C\left(\sum_{i\in\mathbb{N}}\frac{\rho_i}{\sqrt{\alpha}}\right)-1\right)-\sum_{i\in\mathbb{N}}\nu_i\left(\frac{\rho_i}{\sqrt{\alpha}}-p_{i,min}\right). \end{aligned} \tag{24}$$

Then, we can write the function φ in Theorem 6.1 (vii), for any $\vec{d} \in \mathbb{R}^N$, as

$$\varphi_{\vec{\rho}^*(\hat{\vec{\rho}}^1, c(t))}(\vec{d}) = \vec{d}'\frac{\partial^2}{\partial\vec{\rho}^2}L(\vec{\rho}^*(\hat{\vec{\rho}}^1, c(t)), \lambda^*, (\nu_i^* : i \in \mathbb{N}))\vec{d},$$

where λ^* and $(\nu_i^* : i \in \mathbb{N})$ are the optimal Lagrange multipliers and variables. Substituting (24), we have that

$$\begin{aligned} \varphi_{\vec{\rho}^*(\hat{\vec{\rho}}^1, c(t))}(\vec{d}) = \sum_{i\in\mathbb{N}} d_i^2 \Bigg(1 - \frac{1}{\alpha}U''\left(\frac{\rho_i^*(\hat{\vec{\rho}}^1, c(t))}{\sqrt{\alpha}}, \omega_i\right) \\ + \frac{1}{\alpha}\Bigg(2f'\left(\sum_{i\in\mathbb{N}}\frac{\rho_i^*(\hat{\vec{\rho}}^1, c(t))}{\sqrt{\alpha}}\right) \\ + f''\left(\sum_{i\in\mathbb{N}}\frac{\rho_i^*(\hat{\vec{\rho}}^1, c(t))}{\sqrt{\alpha}}\right)\left(\sum_{i\in\mathbb{N}}\frac{\rho_i^*(\hat{\vec{\rho}}^1, c(t))}{\sqrt{\alpha}}\right)\Bigg) \\ + \frac{\lambda^*}{\alpha}C''\left(\sum_{i\in\mathbb{N}}\frac{\rho_i^*(\hat{\vec{\rho}}^1, c(t))}{\sqrt{\alpha}}\right)/c(t)\Bigg). \end{aligned}$$

Since λ^* is the optimal Lagrange multiplier, $\lambda^* \geq 0$. Also U is a strictly increasing, concave function, and C and f are strictly increasing, convex functions. Moreover, $p_i \in \mathbb{P}$ so that ρ_i lies in a closed set $\mathbb{P}_0$, for $i \in \mathbb{N}$. Therefore, there exist positive constants $\xi_{U''}$, $\xi_{f'}$, and $\xi_{f''}$ such that $U''(\rho_i) \leq -\xi_{U''}$, $f'(\rho_i) \geq \xi_{f'}$, and $f''(\rho_i) \geq \xi_{f''}$, for all $\rho_i \in \mathbb{P}_0$. So we have that for any $\vec{d} \in \mathbb{R}^N$,

$$\varphi_{\vec{\rho}^*(\hat{\vec{\rho}}^1, c(t))}(\vec{d}) \geq \left(1 + \frac{\xi}{\alpha}\right)\sum_{i\in\mathbb{N}} d_i^2 > \sum_{i\in\mathbb{N}} d_i^2, \tag{25}$$

where $\xi = \xi_{U''} + 2\xi_{f'} + \xi_{f''}$ is a positive constant. Now, we have verified the condition of Theorem 6.1 (vii) and hence from Theorem 6.1 of [24], Theorem 6.1 (v) is satisfied, which equals to the second-order growth condition. Thus, for proposition 6.1 of [22], both conditions are satisfied. We could use it safely and conclude that:

$$\begin{aligned} \text{dist}(\vec{\rho}^*(\hat{\vec{\rho}}^1, c(t)), \vec{\rho}^*(\hat{\vec{\rho}}^2, c(t))) &\leq \left(1 + \frac{\xi}{\alpha}\right)^{-1}\text{dist}(\hat{\vec{\rho}}^1, \hat{\vec{\rho}}^2) \\ &< \text{dist}(\hat{\vec{\rho}}^1, \hat{\vec{\rho}}^2). \end{aligned}$$

Thus, we can conclude that

$$E\left[\left(\text{dist}(\vec{\rho}^*(\hat{\vec{\rho}}^1, c(t)), \vec{\rho}^*(\hat{\vec{\rho}}^2, c(t)))\right)^2\right] < \left(\text{dist}(\hat{\vec{\rho}}^1, \hat{\vec{\rho}}^2)\right)^2.$$

Further, we have that

$$\begin{aligned} &\text{dist}(E[\vec{\rho}_i^*(\hat{\vec{\rho}}^1, c(t))], E[\vec{\rho}_i^*(\hat{\vec{\rho}}^2, c(t))]) \\ &= \sqrt{\sum_{i\in\mathbb{N}}\left(E\left[\rho_i^*(\hat{\vec{\rho}}^1, c(t)) - \rho_i^*(\hat{\vec{\rho}}^2, c(t))\right]\right)^2} \\ &\leq \sqrt{\sum_{i\in\mathbb{N}}E\left[\left(\rho_i^*(\hat{\vec{\rho}}^1, c(t)) - \rho_i^*(\hat{\vec{\rho}}^2, c(t))\right)^2\right]} \\ &= \sqrt{E\left[\left(\text{dist}(\vec{\rho}^*(\hat{\vec{\rho}}^1, c(t)), \vec{\rho}^*(\hat{\vec{\rho}}^2, c(t)))\right)^2\right]} < \text{dist}(\hat{\vec{\rho}}^1, \hat{\vec{\rho}}^2). \end{aligned}$$

The first inequality is due to Jensen's inequality. This proves our second intermediate result.

Then, suppose that the fixed point equation (21) has two distinct solutions $\hat{\vec{\rho}}^1$ and $\hat{\vec{\rho}}^2$. We have that

$$\begin{aligned} \text{dist}(\hat{\vec{\rho}}^1, \hat{\vec{\rho}}^2) &= \text{dist}(E[\vec{\rho}_i^*(\hat{\vec{\rho}}^1, c(t))], E[\vec{\rho}_i^*(\hat{\vec{\rho}}^2, c(t))]) \\ &< \text{dist}(\hat{\vec{\rho}}^1, \hat{\vec{\rho}}^2), \end{aligned}$$

which is an contradiction. This implies that (21) has at most one solution. We conclude that (20) has a unique solution. ■

We next show the convergence of $\hat{p}_i(t)$ as stated in the following lemma.

Lemma 3: $\hat{p}_i(t)$ converges almost surely to the unique solution $\hat{\vec{p}}$ of the fixed point equation $E[\vec{p}^*(\hat{\vec{p}}, c(t))] = \hat{\vec{p}}$.

Proof: Given that $c(t)$ is a stationary ergodic process, the updating function (17) can be considered as a stochastic approximation update equation. We can apply Theorem 1.1 of Chapter 6 in [25] for the convergence proof. We verify the assumptions in Theorem 1.1 of Chapter 6 in [25] in the following.

We first list the variables used in Theorem 1.1 and correspond them to our problem and our notation style: $\vec{\theta}_t = \hat{\vec{p}}^*(t)$, $\xi_t = c(t+1)$, $(Y_t)_i = \alpha(p_i^*(\hat{\vec{p}}^*(t), c(t+1)) - \hat{p}_i^*(t))$, $\forall\, i \in \mathbb{N}$, $\epsilon_t = \frac{1}{t+\alpha}$, $g(\hat{\vec{p}}, c(t)) = \alpha(p_i^*(\hat{\vec{p}}, c(t)) - \hat{p}_i^*)$, $\forall\, i \in \mathbb{N}$, $\delta\vec{M} = \vec{0}$, $\vec{\beta}_t = \vec{0}$ and $\vec{Z}_t = \vec{0}$ for each t.

Now we need to verify that all the assumptions in Chapter 6 of [25] from (A.1.1) to (A.1.8) are satisfied. According to Property 1, $E[Y_t]$ is a continuous function of $\hat{p}_i^*(t)$ and $\vec{p}_i^*(\hat{\vec{p}}^*(t-1), c(t)) \in \mathbb{P}^N$ for any t. Thus, (A.1.1) is satisfied. (A.1.2) also follows from Property 1 that $g(\hat{\vec{p}}, c(t))$ is a continuous function of $\hat{\vec{p}}$, which guarantees (A.1.7) as well. For (A.1.3), we can take the following form of the function

$$(\bar{g}(\hat{\vec{p}}^*(t)))_i = \alpha(E[p_i^*(\hat{\vec{p}}^*(t), c(t+1))] - \hat{p}_i^*(t)).$$

According to [25], (A.1.3) holds due to the strong law of large numbers, because $c(t)$ is a stationary ergodic process. Since $\vec{\beta}_t = \vec{Z}_t = \vec{0}$ for each t, we have both (A.1.4) and (A.1.5) hold true. For (A.1.6), it holds because $g(\hat{\vec{p}}, c(t))$ is bounded. Hence, all the assumptions are satisfied. It follows Theorem 1.1 in [25] and Property 2 that $\hat{p}_i(t)$ converges almost surely to the unique solution of $E[\vec{p}^*(\hat{\vec{p}}, c(t))] = \hat{\vec{p}}$. ■

Based on the convergence of $\hat{p}_i(t)$, we are ready to prove the asymptotic optimality of the online algorithm, which indicates that for a sufficiently long time period, the time averaged difference between the online and offline objective values will become negligible. We introduce the following lemma for the optimality proof.

Lemma 4: The following limit exits and converges for $i \in \mathbb{N}$:

$$\lim_{T\to\infty}\left(\frac{1}{T}\sum_{t=1}^{T} p_i^*(t) - \hat{p}_i(T)\right) = 0.$$

Proof: Rewrite (17) and sum from $t = 1$ to T. We have

$$\sum_{t=1}^{T}\left(\frac{t+\alpha}{\alpha}\right)(\hat{p}_i(t) - \hat{p}_i(t-1)) = \sum_{t=1}^{T}(p_i^*(t) - \hat{p}_i(t-1)).$$

Expanding the sum on the LHS, it follows that

$$\frac{1}{\alpha}\left(T\cdot\hat{p}_i(T) - \sum_{t=1}^{T}\hat{p}_i(t-1)\right) - (\hat{p}_i(T) - \hat{p}_i(1)) = \sum_{t=1}^{T}(p_i^*(t) - \hat{p}_i(T) + \hat{p}_i(T) - \hat{p}_i(t-1)).$$

Take limit over T on both sides and it follows that

$$\lim_{T\to\infty}\frac{T\cdot\hat{p}_i(T) - \sum_{t=1}^{T}\hat{p}_i(t-1)}{\alpha\cdot T} - \lim_{T\to\infty}\frac{\hat{p}_i(T) - \hat{p}_i(1)}{T} = \lim_{T\to\infty}\frac{1}{T}\sum_{t=1}^{T}(p_i^*(t) - \hat{p}_i(T) + \hat{p}_i(T) - p_i^*(t-1)).$$

The second term of the LHS is zero as $T\to\infty$. Rearranging the terms, we have

$$\lim_{T\to\infty}\left(\frac{1-\alpha}{\alpha}\right)\left(\hat{p}_i(T) - \frac{1}{T}\sum_{t=1}^{T}\hat{p}_i(t-1)\right) = \lim_{T\to\infty}\frac{1}{T}\sum_{t=1}^{T}(p_i^*(t) - \hat{p}_i(T)).$$

Since the sequence $\hat{p}_i(t)$ converges as shown in Lemma 3, $\lim_{T\to\infty}\left(\hat{p}_i(T) - \frac{1}{T}\sum_{t=1}^{T}\hat{p}_i(t-1)\right) = 0$, and the LHS will be zero. Thus the limit on the RHS will also be zero. ■

Based on Lemma 4, we have the following theorem.

Theorem 1: The online optimal solution converges asymptotically and almost surely to the offline optimal solution.

Proof: The proof is equivalent to showing that $\lim_{T\to\infty}\frac{1}{T}(\Psi(\mathbf{p}^*) - \Psi(\mathbf{P}^*)) = 0$ holds true almost surely, where $\mathbf{p}^*$ is online optimal solution and $\mathbf{P}^*$ is the offline optimal solution. Recall that $\lambda^*(t)$ and $\nu_i^*(t)$ are the non-negative multipliers that satisfy the KKT conditions of the online problem (see (18)). We define a new differentiable concave function $\Phi(\cdot)$ as follows:

$$\begin{aligned}\Phi(\mathbf{P}^*) &= \sum_{t=1}^{T}\sum_{i\in\mathbb{N}} U(P_i^*(t),\omega_i(t)) - \sum_{t=1}^{T} f\left(\sum_{i\in\mathbb{N}} P_i^*(t)\right)\sum_{i\in\mathbb{N}} P_i^*(t)\\ &\quad -\frac{\alpha T}{2}\sum_{i\in\mathbb{N}}\mathrm{Var}(\vec{P}_i^*) - \sum_{t=1}^{T}\lambda^*(t)\left(\frac{C(\sum_{i\in\mathbb{N}}P_i^*(t))}{c(t)} - 1\right)\\ &\quad +\sum_{t=1}^{T}\sum_{i\in\mathbb{N}}\nu_i^*(t)(P_i^*(t) - P_{i,min}(t)).\end{aligned} \tag{26}$$

Note that the sum of the first three terms on the RHS of (26) is equal to $\Psi(\mathbf{P}^*)$, while the last two terms on the RHS of (26) are both non-negative. It follows that

$$\Psi(\mathbf{P}^*) \le \Phi(\mathbf{P}^*). \tag{27}$$

Furthermore, with the concave and differentiable properties of function $\Phi(\cdot)$, we have [19]

$$\Phi(\mathbf{P}^*) \le \Phi(\mathbf{p}^*) + \triangledown\Phi(\mathbf{p}^*)\bullet(\mathbf{P}^* - \mathbf{p}^*), \tag{28}$$

where $\bullet$ denotes the inner product operation. Combining (27) and (28), we have

$$\begin{aligned}\Psi(\mathbf{P}^*) &\le \Phi(\mathbf{P}^*) \le \Phi(\mathbf{p}^*) + \triangledown\Phi(p^*)\bullet(P^* - p^*) \qquad (29)\\ &= \sum_{t=1}^{T}\sum_{i\in\mathbb{N}} U(p_i^*(t),\omega_i(t))\\ &\quad - \sum_{t=1}^{T} f\left(\sum_{i\in\mathbb{N}} p_i^*(t)\right)\sum_{i\in\mathbb{N}} p_i^*(t) - \frac{\alpha T}{2}\sum_{i\in\mathbb{N}}\mathrm{Var}(\vec{p}_i^*)\\ &\quad - \sum_{t=1}^{T}\lambda^*(t)\left(\frac{C(\sum_{i\in\mathbb{N}}p_i^*(t))}{c(t)} - 1\right)\\ &\quad + \sum_{t=1}^{T}\sum_{i\in\mathbb{N}}\nu_i^*(t)(p_i^*(t) - p_{i,min}(t))\\ &\quad + \sum_{t=1}^{T}\sum_{i\in\mathbb{N}}(P_i^*(t) - p_i^*(t))\Bigg(U'(p_i^*(t),\omega_i(t)) - g\left(\sum_{i\in\mathbb{N}} p_i^*(t)\right)\\ &\quad + \frac{\alpha}{T}\sum_{k=1}^{T} p_i^*(k) - \alpha p_i^*(t) - \lambda^*(t)\frac{C(\sum_{i\in\mathbb{N}}p_i^*(t))}{c(t)} + \nu_i^*(t)\Bigg).\end{aligned}$$

As $\lambda^*(t)$ and $\nu_i^*(t)$ are the Lagrange multipliers and variables of Prob-ON, we can substitute (18) into the above inequality (29) to have

$$\Psi(\mathbf{P}^*) \le \sum_{t=1}^{T}\sum_{i\in\mathbb{N}} U(p_i^*(t),\omega_i(t)) - \sum_{t=1}^{T} f\left(\sum_{i\in\mathbb{N}} p_i^*(t)\right)\sum_{i\in\mathbb{N}} p_i^*(t) - \frac{\alpha T}{2}\sum_{i\in\mathbb{N}}\mathrm{Var}(\vec{p}_i^*) + \sum_{t=1}^{T}\sum_{i\in\mathbb{N}}\alpha(P_i^*(t)-p_i^*(t))\left(\frac{1}{T}\sum_{k=1}^{T}p_i^*(k)-\hat{p}_i(t-1)\right).$$

Adding $-\hat{p}_i(T)+\hat{p}_i(T)$ to the last component of the RHS of the above inequality, we have

$$\frac{1}{T}\sum_{k=1}^{T}p_i^*(k)-\hat{p}_i(t-1) = \frac{1}{T}\sum_{k=1}^{T}p_i^*(k)-\hat{p}_i(T)+\hat{p}_i(T)-\hat{p}_i(t-1). \quad (30)$$

From Lemma 4, the limit of the above equation is zero for all users. We can take limit of (30) and it follows that

$$\lim_{T\to\infty}\frac{\Psi(\mathbf{P}^*)}{T} \le \lim_{T\to\infty}\frac{1}{T}\left(\sum_{t=1}^{T}\sum_{i\in\mathbb{N}}U(p_i^*(t),\omega_i(t)) - \sum_{t=1}^{T}f\left(\sum_{i\in\mathbb{N}}p_i^*(t)\right)\sum_{i\in\mathbb{N}}p_i^*(t) - \frac{\alpha T}{2}\sum_{i\in\mathbb{N}}\mathrm{Var}(\vec{p}_i^*)\right) = \lim_{T\to\infty}\frac{\Psi(\mathbf{p}^*)}{T}.$$

Thus $\lim_{T\to\infty}\frac{1}{T}(\Psi(\mathbf{P}^*)-\Psi(\mathbf{p}^*)) \le 0$ holds for all users. Because $\mathbf{P}^*$ is optimal to the offline problem and $\Psi(\mathbf{P}^*)$ is the offline objective value, we also have $\Psi(\mathbf{P}^*) \ge \Psi(\mathbf{p}^*)$. We conclude that Theorem 1 holds true. ■

V. PERFORMANCE EVALUATION

A. SIMULATION CONFIGURATION

In this section, we evaluate the proposed online algorithm with trace-driven simulations. The simulation data and parameters are acquired from the traces of power consumption in the Southern California Edison (SCE) area recorded in 2011 [26]. We first study the performance of the proposed algorithm on convergence, grid load variance and peak reduction. We then compare the online algorithm with an existing scheme under different numbers of users.

Consider a power distribution system in a small area with $N = 20$ users and 15 minutes updating periods. Note that a quarter is a practical set which allows DCC to have sufficient time to coordinate all the users so that the system could support more users and that in most cases, 15 minutes is short enough to show the users' change of demand. We will show results within a 24-hour time pattern for an evaluation of the daily operations. We choose users' utility function from a function set $\mathbb{U}$ in which the functions are generated as widely used quadratic expressions (see [5], [6], [8]), with $\omega_i(t) \in (0, 1)$ randomly selected.

$$U(p_i(t),\omega_i(t)) = \begin{cases} \omega_i(t)p_i(t) - \frac{1}{8}p_i(t)^2, & \text{if } 0 \le p_i(t) \le 4\omega_i(t) \\ 4\omega_i(t), & \text{if } p_i(t) \ge 4\omega_i(t). \end{cases} \quad (31)$$

We also assume the basic user demand $p_{i,min}(t)$ and the initial value $p_i(0)$ are selected from the set of $\mathbb{P} = [0.5, 3]$, for all i. The parameters in the energy provisioning cost function (2) are set as $a = 0.05$, $b = c = 0$, and $c(t)$ is selected randomly from the set $\mathbb{C} = [1, 20]$ for each time slot. These parameters are carefully determined after studying the characteristics of the SCE trace. In addition, we choose the price function as

$$f(L(t)) = 0.047 \cdot L(t)^2 - 0.38 \cdot L(t) + 27.67. \quad (32)$$

It is a quadratic function and also a twice-differentiable increasing convex function as discussed in Section II-A.4. This model is formulated from the predicted and actual prices from the SCE trace [27]. We simulate two scenarios with α set as 1 and 0.01, respectively, to examine how it affects the result.

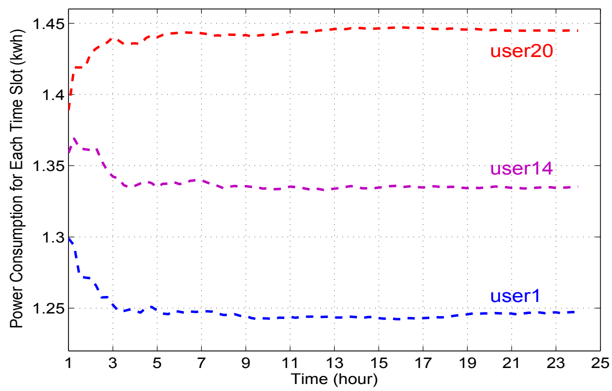

FIGURE 2. Convergence of $\hat{p}_i(t)$ for different users ($\alpha = 1$).

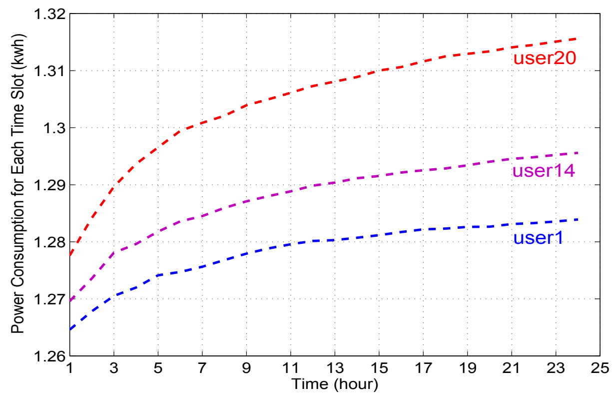

FIGURE 3. Convergence of $\hat{p}_i(t)$ for different users ($\alpha = 0.01$).

B. ALGORITHM PERFORMANCE

We first study the convergence of $\hat{p}_i(t)$. Earlier discussions in Sec. IV show that $\hat{p}_i(t)$ is convergent. Fig. 2 illustrates that for $\alpha = 1$, one day is sufficient for $p_i^*(t)$ to converge to steady state values. In Fig. 3, it takes more time to converge.

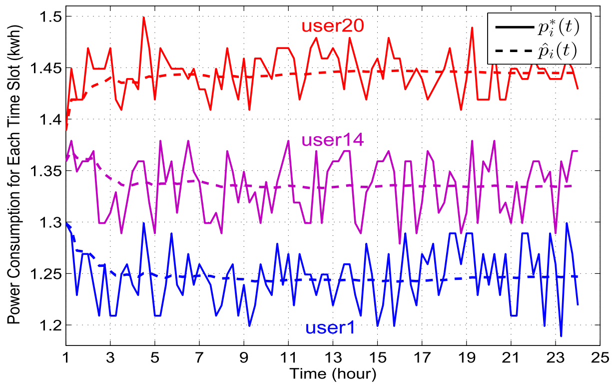

FIGURE 4. **Online power distribution $p_i^*(t)$ and $\hat{p}_i(t)$ for different users when $\alpha = 0.1$.**

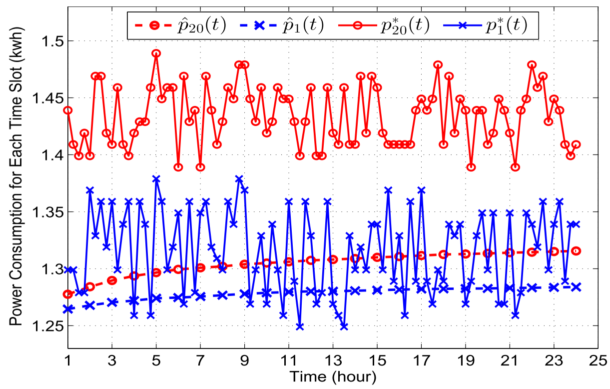

FIGURE 5. **Online power distribution $p_i^*(t)$ and $\hat{p}_i(t)$ for different users when $\alpha = 0.01$.**

In the online problem Prob-ON, α is not only a parameter integrating different objectives, but also an important coefficient affecting the convergence of the algorithm. In the online updating equation (17), it is clear that a large α will cause relatively a large disturbance, especially at the very beginning. However, a large α will also lead to fast convergence, and vice versa, as shown in Figs. 2 and 3. Besides, α also affects the impact of the variance (or, smoothness) on the overall objective value (14). It shapes the grid load curve to some degree, as we will see in Section V-C.

Lemma 4 states that $\hat{p}_i(t)$ will converge to the time averaged $p_i^*(t)$ if we run the simulation sufficiently long. For a larger α, the convergence will be faster, shown in Fig. 4, where we find that $\hat{p}_i(t)$ fluctuates uniformly along the $p_i^*(t)$ curve for different users. For a smaller α, the convergence could be very slow. Fig. 5 demonstrates the slow convergence when $\alpha = 0.01$. However, the convergence of $\hat{p}_i(t)$ is proved to be true as $T \to \infty$ (see the proof of Lemma 4). In Fig. 5, it can be seen that $\hat{p}_i(t)$ is still approaching $p_i^*(t)$, although slowly. Therefore, the value of α should be carefully chosen to trade-off between convergence and other objectives.

More importantly, our main objective is to develop an optimal online algorithm to reduce the variance of the grid load and to balance electricity demand and supply. In Fig. 6, we plot the total power consumption achieved with the online algorithm and the actual load. The real power usage is the summation of 20 independent users' consumption generated by the average real load in the SCE trace on a hot day (i.e., Sept. 1, 2011) [26]. The constraints are derived from the real load in the 2011 SCE trace. For better presentation, we only plot the result of the online algorithm with $\alpha = 1$. The results with $\alpha = 0.01$ will be shown in Section V-C.

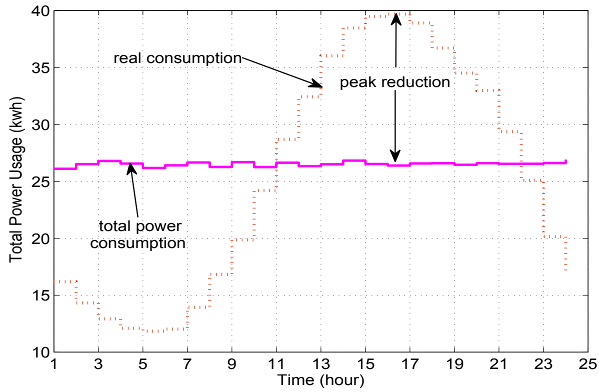

FIGURE 6. **Real power usage and total power usage by the online algorithm when $\alpha = 1$.**

In Fig. 6, we find that the online algorithm achieves a well smoothed grid load. Interestingly, although the power usage of each user varies over time (as shown in Fig. 4), the total power usage is effectively smoothed out by the online algorithm. This result demonstrates the effectiveness of variance detection and reduction of the online algorithm. Although the controlled curve lies slightly above the average level of the real load, it reduces the cost of energy provisioning by achieving a considerable peak reduction, which is about 35% in this scenario with only 20 users.

C. COMPARISON WITH A BENCHMARK

We next compare the online algorithm with the Optimal Real-time Pricing Algorithm (ORPA) presented in [8] as a Benchmark. Comparing to prior work, this one formulates a similar but simpler problem to our problem. It adopts a real-time pricing strategy to maximize social welfare of the smart grid, as

$$\max \sum_{i \in \mathbb{N}} \left(U(p_i(t), \omega_i(t)) - C\left(\sum_{i \in \mathbb{N}} p_i(t) \right) \right), \tag{33}$$

for $t \in \{1, 2, \ldots, T\}$ and for all independent user i. As we can see, (33) is similar to but simpler than (14). With the same parameters as in the online algorithm, this is also a convex optimization problem. We can solve (33) with a centralized interior-point method as discussed in [8].

Firstly, we show the total power consumption of different algorithms in Fig. 7. From the aspect of smoothness, we could see clearly that the online optimal real-time energy distribution algorithm with $\alpha = 1$ (termed OORA(1)) achieves the best performance. The figure also shows that the online algorithm with $\alpha = 0.01$ (termed OORA(0.01)) also outperforms the benchmark ORPA. All the three algorithms achieve smoother total loads than the real consumption (RC). The

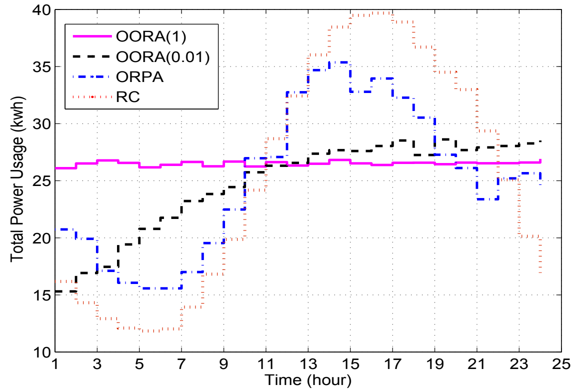

FIGURE 7. Total power consumption for OORA(1), OORA(0.01), ORPA and RC.

peak reductions over RC are 35% for OORA(1), 28% for OORA(0.01), and 12.5% for ORPA. Therefore, OORA(1) achieves the largest peak reduction, while OORA(0.01) still outperforms ORPA with considerable gains.

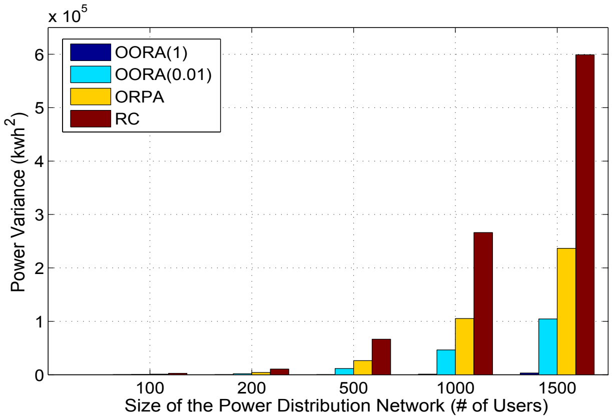

FIGURE 8. Total power variance by OORA(1), OORA(0.01), ORPA and RC.

Next, we plot the variance of the total load in Fig. 8 for different system settings. These results are consistent with that in Fig. 7. We find that OORA(1) achieves the minimum variance for all the cases simulated, while OORA(0.01) still outperforms ORPA with a much smaller variance. This is because variance is explicitly incorporated into the objective function in the online problem formulation, while ORPA is designed mainly to maximize the social welfare as in (33) and cannot guarantee a smooth total grid load.

Finally, we provide a more detailed comparison of the three schemes in Table 1, where the simulation results of several individual performance measures are listed for networks of 200, 500, and 1000 users. Note that the price function is different for different network sizes, which is a function of the total load. As defined in (34), $\overline{V}$, $\overline{U}$, $\overline{F}$, and $\overline{PK}$ denote the averages across users of the total power variance, users' utility, users' cost, and the peak of the total load, respectively, while c is the total energy provisioning cost for the entire period.

TABLE 1. Simulation results of several individual performance measures as defined in (34) for OORA(1), OORA(0.01), ORPA and RC.

Algorithm	N	$\overline{V}$	$\overline{U}$	$\overline{F}$	$c\ (\times 10^3)$	$\overline{PK}$
OORA(1)	200	**0.02**	3.52	3.41	1.69	**1.35**
OORA(0.01)	200	9.3	3.59	3.27	1.61	1.46
ORPA	200	21.5	3.56	3.43	1.54	1.79
RC	200	53.5	3.86	3.65	1.86	2.07
OORA(1)	500	**0.05**	3.53	3.31	10.5	**1.37**
OORA(0.01)	500	23.2	3.63	3.42	10.1	1.51
ORPA	500	52.6	3.54	3.28	9.54	1.83
RC	500	113	3.88	3.61	14.0	2.27
OORA(1)	1000	**0.10**	3.51	3.25	42.2	**1.41**
OORA(0.01)	1000	44.1	3.59	3.30	40.2	1.59
ORPA	1000	105	3.54	3.25	38.1	1.93
RC	1000	266	3.87	4.23	54.1	2.58

$$\begin{cases} \overline{V} = \frac{1}{N}\sum_{i\in\mathbb{N}} \mathrm{Var}(p_i^*(t)) \\ \overline{U} = \frac{1}{N}\sum_{t=1}^{T}\sum_{i\in\mathbb{N}} U(p_i^*(t), \omega_i(t)) \\ \overline{F} = \frac{1}{N}\sum_{t=1}^{T} f(\sum_{i\in\mathbb{N}} p_i^*(t))(\sum_{i\in\mathbb{N}} p_i^*(t)) \\ \overline{PK} = \frac{1}{N}\max_{t\in[1:T]}\sum_{i\in\mathbb{N}} p_i^*(t) \\ c = \sum_{t=1}^{T} C(\sum_{i\in\mathbb{N}} p_i^*(t)). \end{cases} \tag{34}$$

For $\overline{V}$, the best performer is OORA(1), which is consistent with the earlier results. Also, the variance is increasing as the user number grows. For $\overline{F}$, we observe a relatively stable number of the averaged cost on daily electricity consumption for each user. In the first three algorithms, $\overline{F}$ is almost the same while RC always has the largest number because in reality where the RC curve was recorded, supply was always matched to the user demand. This is confirmed by the results of users' utility $\overline{U}$: as users could use electricity freely, they should have the highest satisfaction level. Observing $\overline{U}$ and $\overline{F}$, we see that a higher satisfaction level is achieved with a higher cost. Moreover, it is interesting to see that utility $\overline{U}$ of OORA(1), OORA(0.01), ORPA are almost the same for different numbers of users, with OORA(0.01) being slightly better. This is because, as in ORPA, the utility is incorporated in the objective function of OORA. When α is small, the first two terms in (14) will have larger weights.

For energy provisioning cost c, ORPA exhibits its advantage as it includes this term in the objective function. Also, if we take $\overline{U} - c$, ORPA is also the best performer, which could be expected from its objective function (33). However, this advantage becomes insignificant when the variance $\overline{V}$ and the peak $\overline{PK}$ are considered. OORA has unique advantages on variance control and peak reduction. It is also worth noting that OORA is an online algorithm that requires minimal exchange of control/state information within the grid, while the ORPA results are obtained with a centralized solver assuming accurate global information.

VI. CONCLUSION

In this paper, we present a study of optimal real-time energy distribution in smart grid. With a formulation that captures the key design factors of the system, we first present an offline algorithm that can solve the problem with optimal solutions. We then develop an online algorithm that requires no future information about users and the grid. We also show that the online solution converges to the offline optimal solution asymptotically and almost surely. The proposed online algorithm is evaluated with trace-driven simulations and is shown to outperform an existing benchmark scheme.

REFERENCES

[1] X. Fang, S. Misra, G. Xue, and D. Yang, "Smart grid—The new and improved power grid: A survey," *IEEE Commun. Surv. Tuts.*, to be published.

[2] Y. Huang, S. Mao, and R. M. Nelms, "Adaptive electricity scheduling in microgrids," in *Proc. IEEE Global Commun. Conf.*, Apr. 2013, pp. 1–9.

[3] T. Logenthiran, D. Srinivasan, and T. Z. Shun, "Demand side management in smart grid using heuristic optimization," *IEEE Trans. Smart Grid*, vol. 3, no. 3, pp. 1244–1252, Sep. 2012.

[4] M. Roozbehani, M. Dahleh, and S. Mitter, "Volatility of power grids under real-time pricing," *IEEE Trans. Power Syst.*, vol. 27, no. 4, pp. 1926–1940, Nov. 2012.

[5] D. O'Neill, M. Levorato, A. Goldsmith, and U. Mitra, "Residential demand response using reinforcement learning," in *Proc. IEEE Smart Grid Commun.*, Oct. 2010, pp. 409–414.

[6] P. Samadi, A. H. Mohsenian-Rad, R. Schober, and V. W. Wong, "Advanced demand side management for the future smart grid using mechanism design," *IEEE Trans. Smart Grid*, vol. 3, no. 3, pp. 1170–1180, Sep. 2012.

[7] A. H. Mohsenian-Rad and A. Leon-Garcia, "Optimal residential load control with price prediction in real-time electricity pricing environments," *IEEE Trans. Smart Grid*, vol. 1, no. 2, pp. 120–133, Sep. 2010.

[8] P. Samadi, A. H. Mohsenian-Rad, R. Schober, V. W. Wong, and J. Jatskevich, "Optimal real-time pricing algorithm based on utility maximization for smart grid," in *Proc. 1st IEEE Int. Conf. Smart Grid Commun.*, Oct. 2010, pp. 415–420.

[9] Y. Huang, S. Mao, and R. M. Nelms, "Smooth electric power scheduling in power distribution networks," in *Proc. IEEE Globecom Workshop*, Dec. 2012, pp. 1469–1473.

[10] S. Maharjan, Q. Zhu, Y. Zhang, S. Gjessing, and T. Basar, "Dependable demand response management in the smart grid: A Stackelberg game approach," *IEEE Trans. Smart Grid*, vol. 4, no. 1, pp. 120–132, Mar. 2013.

[11] Y. Zhang, R. Yu, W. Yao, S. Xie, Y. Xiao, and M. Guizani, "Home M2M networks: Architectures, standards, and QoS improvement," *IEEE Commun. Mag.*, vol. 49, no. 4, pp. 44–52, Apr. 2011.

[12] S. Albers, "Online algorithms: A survey," *Math. Program.*, vol. 97, nos. 1–2, pp. 3–26, Jul. 2003.

[13] Z. Zhang and F. Li, "Scheduling unit-length packets with soft deadlines," in *Proc. IEEE Conf. Comput. Commun. Workshop*, Mar. 2010, pp. 1–5.

[14] N. Salodkar, A. Karandikar, and V. Borkar, "A stable online algorithm for energy-efficient multiuser scheduling," *IEEE Trans. Mobile Comput.*, vol. 9, no. 10, pp. 1391–1406, Oct. 2010.

[15] N. Buchbinder, L. Lewin-Eytan, I. Menache, J. Naor, and A. Orda, "Dynamic power allocation under arbitrary varying channels—An online approach," *IEEE/ACM Trans. Netw.*, vol. 20, no. 2, pp. 477–487, Apr. 2012.

[16] V. Joseph and G. de Veciana, "Jointly optimizing multi-user rate adaptation for video transport over wireless systems: Mean-fairness-variability tradeoffs," in *Proc. IEEE INFOCOM*, Mar. 2012, pp. 567–575.

[17] S. Borenstein, M. Jaske, and A. Rosenfeld, *Dynamic Pricing, Advanced Metering and Demand Response in Electricity Markets*. Berkeley, CA, USA: UCEI, Oct. 2002.

[18] R. N. Boisvert, P. A. Cappers, and B. Neenan, "The benefits of customer participation in wholesale electricity markets," *Electr. J.*, vol. 15, no. 3, pp. 41–51, Apr. 2002.

[19] S. Boyd and L. Vandenberghe, *Convex Optimization*. Cambridge, U.K.: Cambridge Univ. Press, 2004.

[20] A. V. Fiacco and Y. Ishizuka, "Sensitivity and stability analysis for nonlinear programming," *Ann. Oper. Res.*, vol. 27, no. 1, pp. 215–236, 1990.

[21] B. Hajek. (2011, Dec.). *An Exploration of Random Processes for Engineers* [Online]. Available: http://www.ifp.illinois.edu/~hajek/Papers/randomprocesses.html

[22] J. F. Bonnans and A. Shapiro, "Optimization problems with perturbations: A guided tour," *SIAM Rev.*, vol. 40, no. 2, pp. 228–264, Jun. 1998.

[23] W. Rudin, *Function Analysis*, 2nd ed. New York, NY, USA: McGraw-Hill, 1991.

[24] J. F. Bonnans and A. D. Ioffe, "Quadratic growth and stability in convex programming problems with multiple solutions," *J. Convex Anal.*, vol. 2, nos. 1–2, pp. 41–57, 1995.

[25] H. J. Kushner and G. G. Yin, *Stochastic Approximation and Recursive Algorithms and Applications*, 2nd ed. New York, NY, USA: Springer-Verlag, 2003.

[26] SCE., Irvine, CA, USA. (2011). *Regulatory Information–SCE Load Profiles–2011 Static Load Profiles* [Online]. Available: http://www.sce.com/005_regul_info/eca/DOMSM11.DLP

[27] CAISO. (2011). *Caiso Daily Report Archives*, Folsom, CA, USA [Online]. Available: http://www.ferc.gov/market-oversight/mkt-electric/california/caiso-archives.asp

YU WANG received the M.E. degree in instrument science and technology and the B.E. degree in measuring and control technology and instrumentation from Southeast University, Nanjing, China, in 2011 and 2008, respectively. Since 2011, he has been pursuing the Ph.D. degree with the Department of Electrical and Computer Engineering, Auburn University, Auburn, AL, USA. His current research interests include smart grid and optimization.

SHIWEN MAO (S'99–M'04–SM'09) received the Ph.D. degree in electrical and computer engineering from Polytechnic University, Brooklyn, NY, USA. Currently, he is the McWane Associate Professor with the Department of Electrical and Computer Engineering, Auburn University, Auburn, AL, USA. His current research interests include cross-layer optimization of wireless networks and multimedia communications, with current focus on cognitive radios, femtocells, 60 GHz mmWave networks, free space optical networks, and smart grid. He is on the Editorial Board of the IEEE TRANSACTIONS ON WIRELESS COMMUNICATIONS, the IEEE INTERNET OF THINGS JOURNAL, the *IEEE Communications Surveys and Tutorials*, and several other journals. He received the 2013 IEEE ComSoc MMTC Outstanding Leadership Award and the NSF CAREER Award in 2010. He is a co-recipient of the IEEE ICC 2013 Best Paper Award and the 2004 IEEE Communications Society Leonard G. Abraham Prize in the Field of Communications Systems.

R. M. NELMS (F'04) received the B.E.E. and M.S. degrees in electrical engineering from Auburn University, AL, USA, in 1980 and 1982, respectively. He received the Ph.D. degree in electrical engineering from Virginia Polytechnic Institute and State University, Blacksburg, VA, USA, in 1987. He is currently a Professor and Chair with the Department of Electrical and Computer Engineering, Auburn University. His current research interests include power electronics, power systems, and electric machinery. In 2004, he was named an IEEE Fellow "for technical leadership and contributions to applied power electronics." He is a Registered Professional Engineer in Alabama.